Received: 3 March 2021 | Revised: 26 April 2021 | Accepted: 14 May 2021

DOI: 10.1111/aor.14002

MAIN TEXT ARTICLE

Artificial Organs WILEY

Reparative effect of super active platelet combined with allogeneic bone for large bone defects

Qinglong Wang | Zhipeng Huang | Xi Huang | Tao Zhang | Wenbo Wang

Department of Orthopedics, the First Affiliated Hospital of Harbin Medical University, Harbin, China

Correspondence
Wenbo Wang, The First Affiliated Hospital of Harbin Medical University, 23 You Zheng Street, Harbin 150001, China.
Email: wenbowang1967@163.com

Funding information
This work was supported by Postgraduate Research & Practice Innovation Program of Harbin Medical University (grant number YJSKYCX2019-39HYD)

Abstract

In clinical practice, autologous bone transplantation is usually used to treat large-scale bone defects. However, autologous bone can cause complications such as secondary injury to patients, the scarcity of autografts. In this study, the study of using super active platelet lysate (sPL) and allogeneic bone to treat the 15 mm long bone defect in right radius of rabbits, and provide an experimental basis for the next step of clinical bone defect treatment. The critical-size defect of New Zealand white rabbits was made and divided into three groups: autologous bone group, allogeneic bone group, and sPL group. They were euthanized 1, 2, and 3 months after the operation, perform imaging and histological observation on the repair of bone defect area. The results showed that there were varying degrees of new bone in the bone defect. CT data showed that the bone defect repair rate and new bone mass in each group increased month by month (P <.05). Bone tissue (BV) and bone tissue to the total volume (BV/TV, %) in the sPL group > allogeneic bone group, autologous bone group > allogeneic bone group, with statistical significance (P < .05). Compared with the allogeneic bone group, the sPL group can significantly promote the healing of bone defects, enhance the bone density after fracture healing. The repair effect after 3 months was similar to that of the autogenous bone group. The use of allogeneic bone and sPL therapy may become part of a comprehensive strategy for tissue engineering to treat bone defects.

KEYWORDS

allogeneic bone, bone grafts, large bone defect, platelet lysate, PRP

1 | INTRODUCTION

The treatment of large segmental bone defects caused by acute high-energy trauma, tumor destruction, or resection after infection is a significant challenge for orthopedic surgeons.[1-3] If the bone defect exceeds a certain volume, the body itself cannot be repaired, the weight-bearing and conduction function of the bone is lost, and normal joint activities cannot be completed, which brings obstacles to the function of the limbs. Due to the difficulty of treating these defects and poor therapeutic outcomes of current therapies, these bone defects often present delayed or absent healing.[4] The current methods used to treat large segmental bone defects include autologous bone transplantation, bone allografts, and vascularized bone grafts.[5,6] Autologous bone grafts are considered the gold standard for treating bone defects smaller than 5 cm, this is due to their osteogenic and osteoinductive properties, and their osteoconductivity.[7] However, they have

a limited supply of donors, complicated procedures, and often persistent pain at the harvest site, as well as potential infection.[7-12] Vascularized free bone transfers also have various disadvantages,[1,13] such as osteonecrosis.[14] An alternative method is to perform bone allografts, which help retain the inherent osteoconductive properties and minimize the spread of donor-host disease. However, the osteoinductive ability of processed (frozen or freeze-dried) allogeneic bone is still uncertain; as the osteoprogenitor cells are destroyed during tissue processing. As a result, the osteoinductive material is only partially retained, which may result in suboptimal clinical effects.[15,16] In this study, we achieved promising effects using autologous bone grafts in a simple surgical method.

Recently, research in the use of platelet-rich plasma (PRP) has been gaining momentum in the field of bone regeneration and is being employed extensively in orthopedic surgery.[17] PRP is a blood product with a higher concentration of platelets than physiological whole blood and has been proven to be a powerful tool for tissue repair,[18,19] PRP contains various important GFs that enable the growth of bone and even though the mechanism of the bone regeneration is not well understood presently, its ease of handling and application makes it a good agent in the orthopedic field.[20] PRP is considered a suitable method to treat bone defects when used in combination with certain specific biological materials, such as bovine-derived hydroxyapatite, bovine porous bone mineral (BPBM), and bio-guide membrane (BGM).[21,22]

Super activated platelet lysate (sPL) is an innovative platelet lysate based on traditional platelet-rich technology. Unlike PRP, sPL does not require platelet activation, and it can be injected directly into bone defects. Moreover, sPL has the function of PRP to repair bone defects.[23] Therefore, this study aimed to verify the osteogenic effect of sPL combined with allogeneic bone, and compared it to that of pure autologous bone transplantation and pure allogeneic bone transplantation.

2 | MATERIALS AND METHODS

2.1 | Allogeneic bone preparation

Fifty-four male New Zealand white rabbits at 6 months old, weighing about 3.0kg, bred in a standard specific pathogen-free (SPF) laboratory were used. Fifty rabbits were used as experimental animals and four rabbits were sacrificed by anesthesia (ketamine and isoflurane) for the preparation of allogeneic bone. Under aseptic conditions, the bilateral iliac bones and femoral condyles were removed and the soft tissue and periosteum on the bone surface were removed. These were then trimmed into long strips of 15 mm × 4 mm × 3 mm after simple washing. The allogeneic bone was rinsed repeatedly with normal saline until the bone marrow became white in appearance. Allogeneic bone was stored in a refrigerator at 4°C for 30 minutes, frozen at −20°C for 12 hours, and then stored at −80°C for 7 days. After removal from the freezer, allogeneic bone was treated with anhydrous ethanol-chloroform (1:1 mixture) and freeze-dried. It was then sterilized with ethylene oxide and sealed at −20°C.

2.2 | sPL preparation

In order to prevent immune rejection, the blood of each animal was used to extract sPL.[23] In all experimental rabbits, venous blood was taken from the ear vein and mixed with an appropriate amount of sodium citrate solution. PRP was prepared by the secondary centrifugation method: the first centrifugation was conducted at 1000 *g* for 15 minutes. Most of the red blood cells in the bottom layer were discarded. The second centrifugation was conducted at 1866 *g* for 8 minutes. Then the sPL was prepared. Prepared PRP was repeatedly frozen and thawed at −80°C/37°C three times, and then centrifuged again at 2300 *g* for 30 minutes. The supernatant was filtered with a 0.22 μm sterile filter membrane to collect the sPL. In all experiments, 1 mL of sPL was prepared and stored at −80°C. In order to determine the levels of various growth factors present in the PRP preparation, the concentrations of IGF-1, bFGF, VEGF, and PDGF were determined by ELISA according to manufacturer's instructions (Jiangsu Jingmei Biotechnology co., Ltd., Yancheng, China).

2.3 | Surgical procedures and sPL injection

All animal experiments and care procedures were approved by the Ethics Committee of Laboratory Animal Ethics Committee of the First Affiliated Hospital of Harbin Medical University. Fifty rabbits were randomly divided into three groups, autogenous bone group ($n = 17$), allogeneic bone group ($n = 17$, allogeneic bone + saline), and sPL group ($n = 16$, allogeneic bone + sPL). Briefly, the experimental rabbits were weighed and then anesthetized with ketamine and under anesthesia through inhalation of isoflurane. The experimental rabbits were fixed in the supine position. Each rabbit was aseptically and anesthetized by local injection of lidocaine after marking the skin on the right forelimb. Surgery was conducted in accordance with published protocols.[24] A 4 cm vertical skin incision was made in the middle of the right radius to superficial the surface fascia and expose the radius from the tendon space. A 15 mm long bone defect was formed by osteotomy in the middle of the right radius. When performing the osteotomy, attention was paid to protect the contralateral ulna, evaluate the integrity of the ulna after osteotomy, and mark the bone defect site

with a marker on the skin. In the autogenous bone group, the contralateral iliac bone was removed and trimmed into a long strip of bone about 15 mm × 4 mm × 3 mm. After implanting the bone graft materials in each group, they were rinsed with diluted iodophor water, covered with antibiotics, and the superficial fascia and skin were carefully sealed layer by layer with four to zero sutures using conventional procedures. On the third postoperative day, 0.5 mL sPL or 0.5 mL normal saline was directly injected into the bone defect in the sPL group and the allogeneic bone group, respectively, according to the skin markers. During injection, the needle punctured the soft tissue of the ulnar side of the bone graft. Before injection of sPL, we ensured there was no blood sucked back up the syringe and that there was no overflow or leakage after injection.

If infection control was ineffective or rabbits died, they were excluded from the experiment. Each month for 3 months, 15 rabbits were euthanized by aeroembolism. The ulna and radius bones were removed from the surgical site to assess the blood supply and morphological changes of the implants, and fixed in a 4% paraformaldehyde solution.

2.4 | Analysis of bone formation

During the wound healing process, the rabbit's mental state, diet, and incision healing were constantly observed. We also a'ssessed whether there was an infection in the radius area, the peripheral blood supply, and any morphological changes after repair.

After washing the fixed bone specimen with normal saline, a small animal Micro-CT (Quantum GX2 micro-CT imaging system, Perkinelmer, USA) was used to scan the radius and ulna around the bone defect at a frequency of 90 kV and 88 μA along the long axis.

According to a scoring scale based on cortical regeneration and acceleration of healing after surgery,[25] using the radiographic scoring scale of Garrett et al in Table 1 for evaluation, and randomly select three slices for blind evaluation of the CT results of each time period. Blind evaluations were conducted by three medically trained researchers.

Using the Micro-CT analysis software Analyze14.0 (Biomedical Imaging Resource at Mayo Clinic), we selected the region of interest (ROI), and reconstructed a cylindrical area with a diameter of 6 mm and a height of 15 mm in the center of the bone repair, and as far as possible from the ulna. We reconstructed the axial image into a 3D image to measure the volume of bone tissue (BV), the percentage of bone tissue to the total volume (BV/TV, %), the relative volume ratio, and the number of trabeculae (Tb.N, 1/mm), trabecular bone thickness (Tb.Th, mm), trabecular separation (Th. Sp, mm), and bone density (BMD, mg/cc). When using a complete columnar bone graft or allogeneic bone graft, we used the same size of the implanted tissue implantation. However, it was still difficult to determine new bone formation in the graft bone injury area through CT scans or radiological evaluation. Therefore, our analysis of new bone formation through these methods was limited.

After the CT examination, 10% EDTA was added for decalcification, and then 20 mm long tissues were cut from the rabbit radius containing the defect area at the center. The cut specimens were embedded in paraffin, with the radius defect area at the center. The defect repair area was cut along the longitudinal axis of the bone shaft to a section length of about 20 mm and thickness of 5 μm. HE and Masson staining were used to assess bone healing, observed under an optical microscope.

2.5 | Statistical analysis

All measurement data are expressed as mean ± standard deviation (x ± s), the experimental groups were analyzed by two-way analysis of variance to assess statistical significance. A P value <.05 was considered statistically significant.

TABLE 1 Radiographic scoring scale according to Garrett et al[25]

Score	Definition
0	No bridging, no callus formation
1	No bridging, initiation of a small amount callus
2	No bridging, obvious callus formation near fracture
3	No bridging, marked callus formation near and around fracture site
4	Rebridging of at least one of the cortices, marked callus formation near and around fracture site
5	Rebridging of at least one of the cortices, marked and complete callus formation around fracture site
6	Rebridging of both cortices, and/or some resolution of the callus
7	Clear rebridging of both cortices and resolution of the callus

TABLE 2 Concentrations of biological factors in the sPL

	PDGF	bFGF	TGF	VEGF
sPL	756.7 ± 71.2 ng mL^{-1}	416.4 ± 57.0 pg mL^{-1}	32.0 ± 0.7 ng mL^{-1}	25.84 ± 0.7 ng mL^{-1}

3 | RESULTS

3.1 | Concentrations of various growth factors in sPL

We first measured the protein concentrations of various growth factors in sPL by ELISA (Table 2).

3.2 | Phenotypic features of the repairs of bone defects

The bone defect was 15 mm, the intraoperative osteotomy of the bone graft was implanted, and the bone was taken to meet the requirements of our study (Figure 1A). The immediate postoperative CT scan showed that the bone graft could be visualized, the bone defect was in a good position, and the ulna was intact (Figure 1B). No local redness, swelling, edema, or dehiscence was observed in the incision site. Two weeks after the operation, no infection or inflammation was observed in the surrounding tissues.

There were varying degrees of new bone formation within the bone defect at each time period. One month following the operation, obvious new bone wrapping and bridging were observed around the bone graft in the sPL group, which was similar to the autologous bone group. Two months following the operation, both the autogenous bone group and the sPL group showed blood vessel ingrowth. (Figure 2) The allogeneic bone group did not show pedicle ingrowth, while this group showed significantly smaller bone graft compared to a previous assessment. (Figure 3) Three months following the operation, the radii of rabbits in the autogenous bone group and the sPL group were intact and regularly shaped, and the bone marrow cavity was formed in some bone tissues. In the allogeneic bone group, vascular pedicles formed, some experimental bone grafts were still visible, and the radius was irregular after the repair.

3.3 | 3D reconstruction of a CT scan image

One month after the operation, the allogeneic bone group showed the bone graft with some new bone formation surrounding it, new bone wrapped around the osteotomy, and no obvious new bone bridging on the middle bone graft (Figures 4 and 5). In the sPL group, there was a large amount of new bone formation surrounding the bone

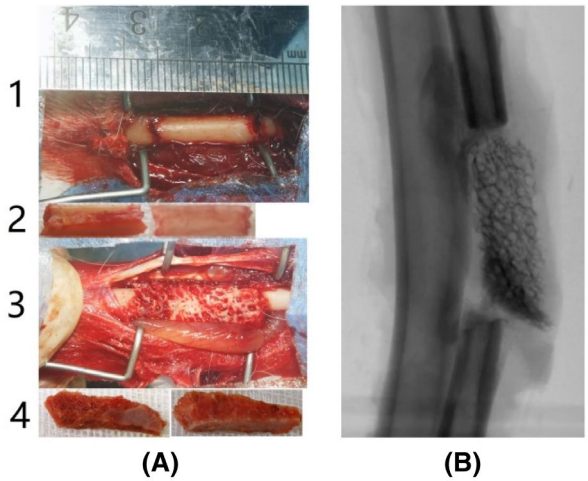

FIGURE 1 A1, Intraoperative osteotomy. A2, The resected radius anteroposterior position. A3, The intraoperative implanted allograft. A4, Anteroposterior position of the iliac bone autograft. B, X-rays image after implantation immediately [Color figure can be viewed at wileyonlinelibrary.com]

defect, which bridged the defect and the bone graft. These phenomena were similar to those observed in the autogenous bone group.

In the allogeneic group, significant reductions in the volume and density of the bone graft were observed after 2 months, compared to those present 1 month after the operation. A large amount of new bone was observed at both ends of the osteotomy, and new bone was seen on the middle bone graft. In the autogenous and the sPL groups, most of the bone graft in the experimental rabbit bone defect was completely absorbed. However, the allogeneic group presented a significantly reduced gap between the fracture ends, irregular radius, unclear bone shape, and no obvious bone marrow cavity.

Three months after the operation, we found that some bone grafts were still present in rabbits from the allogeneic group. This group presented an incomplete radius, no new bone in the middle of the defect, a defect still evident, and there was bone formation around the bone defect. The density of the graft was significantly lower than that of the cortical bone. The radii of rabbits in the autogenous and sPL groups were intact and remodeled. The implanted bone grafts were completely absorbed. Parts of the defect were completely connected with the bone graft, while the peripheral bone cortex was fully connected, and the bone marrow cavity was reopened.

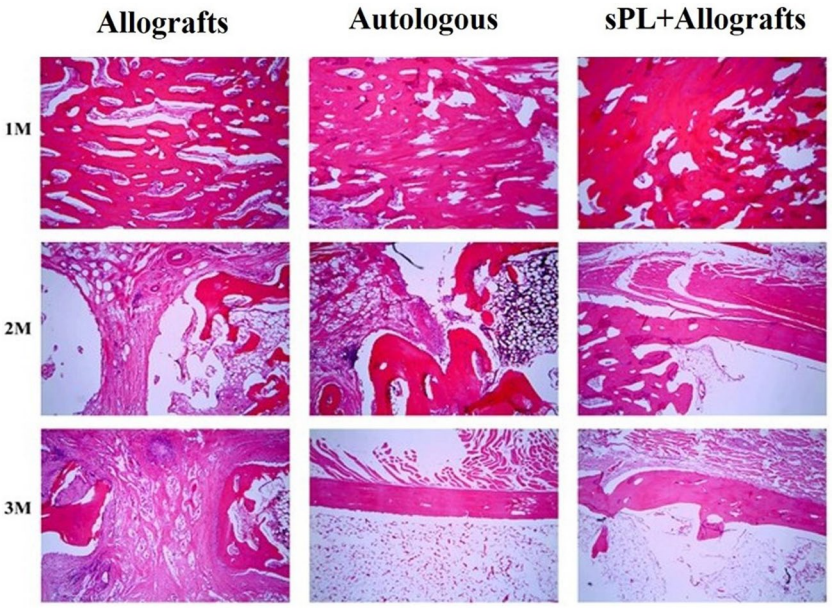

FIGURE 2 HE staining (40X) of the bone in radial bone defect at 1, 2, 3 months after surgery [Color figure can be viewed at wileyonlinelibrary.com]

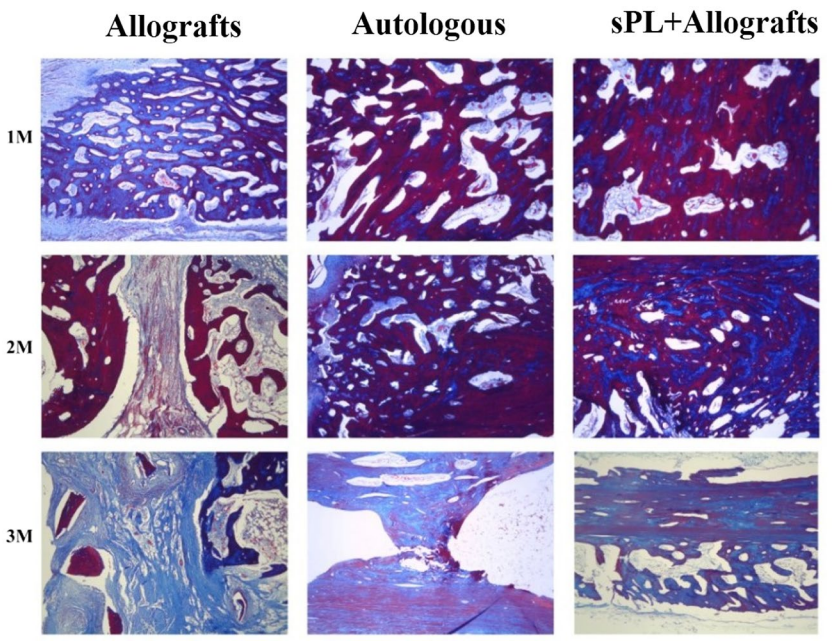

FIGURE 3 Masson staining (40X) of the bone in radial bone defect at 1, 2, 3 months after surgery [Color figure can be viewed at wileyonlinelibrary.com]

3.4 | Data analysis after reconstruction

Compared with simple allogeneic bone transplantation, sPL combined with allogeneic bone transplantation and autologous bone transplantation (positive control group) showed enhanced bone reparative ability (Figure 6A,B). In these groups, the volume of new bone increased monthly ($P < .05$). The volume of new bone observed in the sPL group was the highest for each period, among all groups. The bone tissue (BV) and the percentage of bone tissue to the total volume (BV/TV, %) of the autologous bone group and sPL group were significantly higher compared to the allogeneic bone group ($P < .05$). Three months after surgery, the BV and BV/TV of the sPL group were also significantly higher compared to those of the allogeneic bone group across all months ($P < .05$).

The number of trabeculae (Tb.N, 1/mm) of the autogenous bone group and sPL groups was consistently higher than that of the allogeneic bone group ($P < .05$; Figure 6C–E). However, 3 months after the operation, the Tb.N of the three groups was significantly lower compared to that observed at 2 months ($P < .05$). There was no significant difference between the autogenous bone group and the sPL group. The trabecular bone thickness (Tb.Th, mm) of each group increased monthly ($P < .05$). The thickness of the new bone trabecula of the sPL group was the highest among all groups. Two months after the operation, the Tb.Th of the bone tissue of the sPL group was significantly increased compared with that

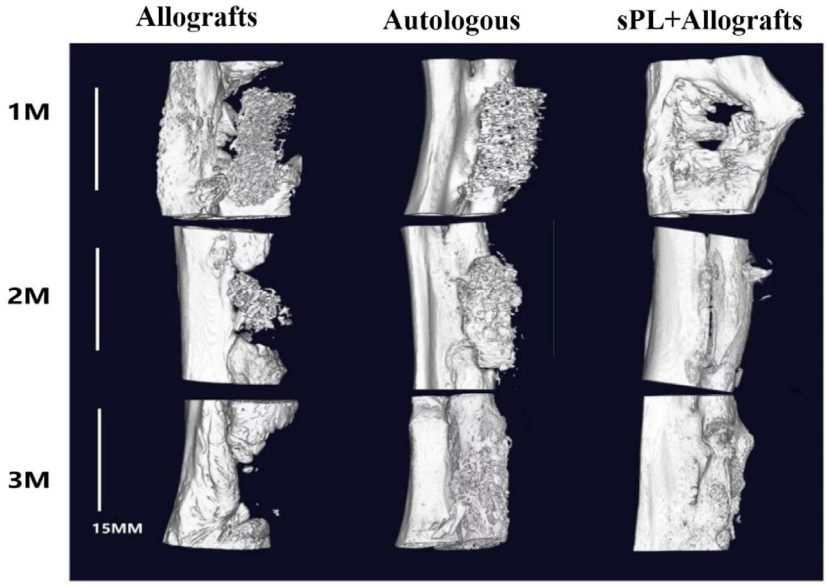

FIGURE 4 Micro-CT 3D reconstruction images of allografts, autogenous, and sPL groups were performed at the time of 1, 2, and 3 months postoperatively [Color figure can be viewed at wileyonlinelibrary.com]

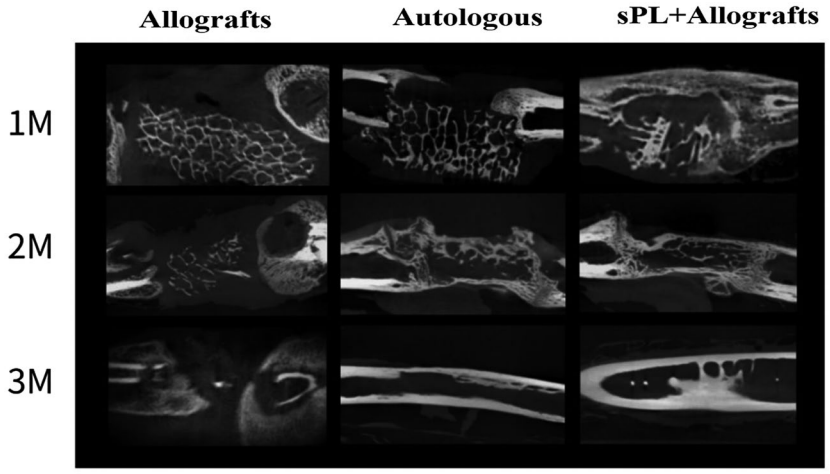

FIGURE 5 Micro-CT 3D reconstructed long axis of radius images of allografts, autogenous, and sPL groups were performed at the time of 1, 2, and 3 months postoperatively

of the autogenous bone group ($P < .05$). Three months after surgery, there was no significant difference in the bone tissue Tb.N, Tb.Th, and trabecular bone spacing (Th. Sp, mm) of the sPL group compared with those of the autogenous bone group. The Tb.Sp of the autogenous bone group and sPL group was significantly lower than that of the allogeneic bone group 1 month after the operation ($P < .05$). Two months later, there was no significant difference in Tb.Sp among the three groups.

The bone density (BMD, mg/cc) of the autogenous bone group and the sPL group showed a monthly increase after the operation ($P < .05$; Figure 6F). In the allogeneic bone group, BMD was increased 2 months after the operation and there was no significant difference compared to 3 months after the operation. At 1 month and 2 months after surgery, there were no significant differences in the BMD among the three groups. Only at 3 months after surgery, the BMD of the autologous bone and sPL groups showed a significant increase compared with that of the allogeneic group ($P < .05$). There was no significant difference in the BMD between the autogenous bone group and the sPL group.

Based on cortical bridging connection and acceleration of healing, in the radiological analysis of bone healing ability, the autologous bone and the allogeneic bone + sPL group showed a better biological effect than the allogeneic bone group in terms of bone formation. The radiology score at 1, 2, and 3 months after surgery were: allogeneic bone: 2.33 ± 0.47, 3.67 ± 0.47, 4.67 ± 0.47; autogenous bone: 3.33 ± 0.47, 5.33 ± 0.47, 6.33 ± 0.47; autogenous bone $\pm$ sPL group: 4 ± 0.82, 7, 7; bone defect with time delay gradually healed, the difference between autologous bone and autologous bone $\pm$ sPL was significantly reduced (Figure 7).

3.5 | Histological analysis

One month after the operation, the areas of HE red staining and Masson's trichrome staining (immature bone) in the

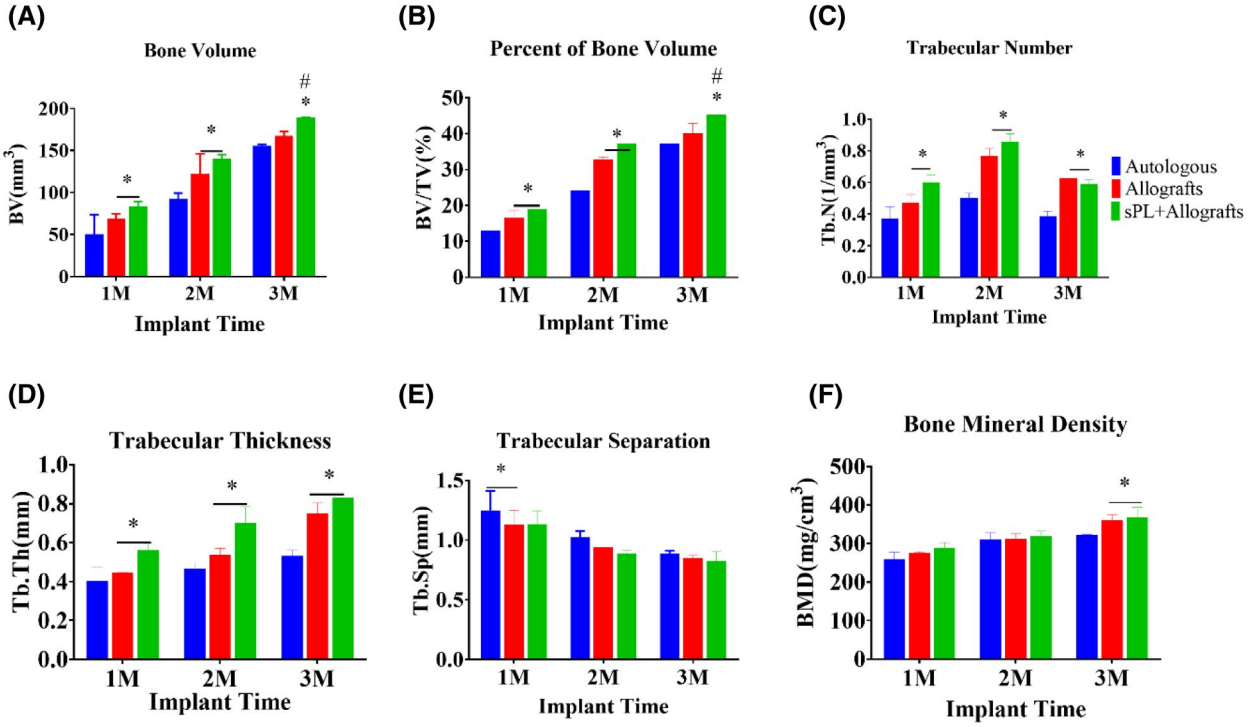

FIGURE 6 Quantitative analysis of Micro-CT of the bone in radial bone defect at 1, 2, 3 months after surgery: (A) BV; (B) BV/TV; (C) Tb.N; (D) Tb.Th; (E) Tb.Sp; (F) BMD; $n = 5$, $^{*}P < .05$ vs Allografts group; $^{\#}P < .05$ vs Autologous group [Color figure can be viewed at wileyonlinelibrary.com]

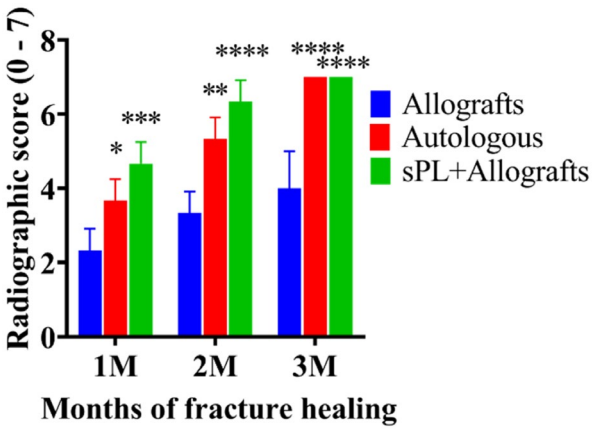

FIGURE 7 The fracture healing was evaluated by Micro-CT, and the imaging evaluation results of the first, second, and third months after the bone defect. Evaluation was carried out by three independent researchers according to Garrett et al's scoring scale, and the results were expressed as the average score ± standard deviation, $^{*}P < .05$ [Color figure can be viewed at wileyonlinelibrary.com]

sPL and autologous bone groups were significantly larger than those of the allogeneic bone group (Figures 2 and 3). Moreover, the trabecular bone was more developed.

Two months after the operation, a large number of new immature bones and fibrous scar tissues were seen at both ends of the defects of the allogeneic bone group. In the autogenous bone group and the sPL group, the Masson red-stained area was reduced compared with that of the previous month. There was an evident bone connection between the broken end of the defect and the original cortical bone, as well as new bone in the medullary cavity of the defect area.

Three months after the operation, the continuity of the radius in the allogeneic bone group was interrupted. There was negligible residual graft wrapped by the immature bone in the middle section, and increased mature bone and closed medullary cavities at the defect end. The continuity of the radius was restored in of the autogenous bone and the sPL groups. Part of the radius was significantly reshaped, the Masson red stained area was reduced, the broken end defect and the original cortical bone was intact, and the medullary cavity was formed in the autogenous bone and the sPL groups. Furthermore, we observed the formation of new bone in these groups. Notably, HE staining reiterated our CT observations. Masson's results suggested that the time required for bone maturation during bone repair in the autogenous bone group and sPL group was shorter when compared to that of the allogeneic group.

4 | DISCUSSION

In a 10-year fracture case registration study, 0.4% of the cases presented obvious bone loss,[26] however, these defects

could delay healing or develop into nonunion. Patients with long bone defects often suffer pain, peripheral joint stiffness, loss of motor function, and disability. The treatment of long bone defects is still patent in the medical field. Autologous bone transplantation is considered a reliable operation, but the availability of the donor site is limited. Possible complications include unreliable graft hypertrophy, late graft fracture, and donor site complications. At present, there have been many animal studies exploring the use of PRP and its derivatives alone or in combination with artificial bone. Moreover, PRP has been used in clinical research to investigate its therapeutic benefit to prevent delayed bone healing. However, there are no effective clinical measures for large bone defects. Therefore, we aimed to investigate PRP derivatives and the therapeutic effects of sPL combined with allogeneic bone. Studies into the osteogenic role of PRP have provided conflicting evidence, and some authors have expressed their views and concerns.[27] It is thought that more standardization is required when preparing and administering PRP to repair bone defects. Without standardization we can never determine the exact roles of PRP and whether it can promote bone healing when used alone or in combination with different bone graft materials. Moreover, the same planting is better than heterogeneous research, and PRP extracted from the whole blood of an animal needs to be used on the same animal. A study[28] highlighted that rabbits are a suitable model for PRP research physiology is similar to that of humans (the average platelet count of rabbits is 400 000/mm^3). Therefore, rabbits were selected as experimental animals in the design of this study. The sPL was obtained from the venous blood of rabbits and contained a variety of biologically active osteogenic factors. For example, PDGF-BB can rescue bone marrow mesenchymal stem cell proliferation, promote angiogenesis, impair osteogenic function, and has a significant effect on the treatment of bisphosphonate-related osteonecrosis of the jaw.[29] bFGF may also restrict stem cell differentiation in vitro. BFGF combined with bioabsorbable hydrogel is a promising tool to help bone regeneration in the skull defect area.[30] VEGF plays an important role in the osteogenesis of cartilage and periosteum, bone development, and bone repair. The response of exogenous VEGF observed in two different model systems and species shows that the VEGF sustained release agents used locally in the bone injury sites are an effective therapy to promote human bone repair.[31]

Due to the fibrous connection at the proximal and distal ends of the ulna and radius, the proper tension of the bone graft implantation, and no requirement to perform internal or external fixation around the bone defect,[32] the radius was selected as the site of the bone defect. The length of segmental bone defect in this study was 1.5 cm and represented −20% of the entire length of a rabbit femur (−7 cm); this corresponded to an −9 cm defect in a human adult femur (−45 cm).[33] In previous studies, there were differences in the selection of experimental rabbits and experimental conditions (such as their age, length of the radius defect, and observation time). In order to observe the entire bone healing process, we chose to observe rabbits for 3 months following surgery.

Autologous bone transplantation is the current "gold standard" for bone grafting. Here, we used 6-month-old male New Zealand rabbits middle radius bone defects. The new bone growth and volume in the sPL group was similar to a tissue engineered bone scaffold equipped with platelet-rich fibrin and nano-biphasic calcium phosphate.[34] BV/TV in the experimental group increased monthly for 3 months. Van Gieson staining confirmed this observation and demonstrated that the new bone around the scaffold was firmly attached. This is consistent with previous research.[35]

The absorption of allogeneic bone implanted in this study was correlated with the degradation of the scaffold. The addition of platelet-rich fibrin accelerated the formation of new bone and the degradation of the scaffold. However, only observational analyzes could be performed. The CT value of the tissue engineered bone used in this study did not reach the CT threshold to be considered new bone. At 1 and 2 months after the operation, Tb.N and Tb.Th of the sPL group were significantly higher compared to those of the allogeneic bone group. Tb.Sp was significantly lower compared to that of the allogeneic bone group. Three months after the operation, the radii in the sPL group and the autogenous bone groups recovered and the bone marrow cavity were developing or completely developed. In the allogeneic group, the bone defect was not completely repaired, the radius still had a bone defect of 4-8 mm, and there was no bone marrow cavity formation. This indicated that sPL combined with allogeneic bone transplantation accelerated the formation of new bone in the early stages of long bone defect repair. Whether the formation of marrow cavity is related to the speed of bone repair requires further study. The microstructure of the new bone in the early stages of bone defect repair was similar to what has been observed previously upon PRP treatment of tibial bone defects in rats.[36] This study showed that the Tb.N and Tb.Th of the PRP treatment group were significantly higher compared to those of the control group. Forty-two days following surgery, there were also relative changes in the Tb.Sp As the tibial bone defects in the above study were nonsegmental, the healing period was shorter than the one presented in our study.[36]

We showed that the Tb.N of the sPL and autogenous bone groups decreased significantly over time, which indicates that the bones were fully matured in the later stages of bone formation, and there was no obvious new bone formation. We proved that platelet analogs can promote bone healing, which was consistent with the results of previous studies.[37] During the experiment, we found that most rabbits in the sPL

and autologous groups were able to stand up, and a small number could only crawl. The weight-bearing behavior may be one of the reasons for the formation of the bone marrow cavity. Therefore, in follow-up research, the surgical operation should be meticulous, the tendon damage and interference should be reduced, the experimental design should be optimized, and multi-factor analysis of bone marrow cavity formation should be conducted.

There are several limitations to this study. First, although the results of this study provide a theoretical basis for repairing bone defects of critical size, further research is needed to determine the effect of hyper-activated platelet lysate combined with allogeneic bone in human patients. Second, it is impossible to standardize the platelet lysate, because there is no uniform standard for platelet lysate; third, we cannot determine the appropriate size of bone tissue and the amount of super activated platelet lysis for repairing critical-size bone defects. We need to conduct further research on the amount of bone and platelets of different sizes to determine the appropriate concentration for transplantation to repair defects of a specific size.

5 | CONCLUSIONS

In conclusion, the therapeutic effects of sPL combined with allogeneic bone transplantation were better compared to allogeneic bone transplantation alone and were comparable to autologous bone transplantation. Moreover, the fracture healing time was similar, and the bone density of the final healing radius defect area was higher compared to the autogenous bone. In cases where there are a large number of bone defects and limited autologous bone acquisition, sPL combined with allogeneic bone grafting may be a suitable candidate therapy for repairing long bone defects. Nevertheless, further research is needed to clarify the osteogenic mechanism of sPL and verify its effects on long bone defects in clinical applications.

CONFLICT OF INTEREST

The author(s) declared no potential conflict of interest with respect to the research, authorship, and/or publication of this article.

AUTHORS' CONTRIBUTIONS

Qinglong Wang performed the experiments, statistical analysis, and drafted the manuscript. Zhipeng Huang helped with the animal experiment. Xi Huang participated in the statistical analysis. Zhipeng Huang, Xi Huang and Tao Zhang participated in the statistical analysis and helped to draft the manuscript. Wenbo Wang designed the experiment, checked the language and structure of the manuscript.

REFERENCES

1. Pobloth AM, Schell H, Petersen A, Beierlein K, Kleber C, Schmidt-Bleek K, et al. Tubular open-porous beta-tricalcium phosphate polycaprolactone scaffolds as guiding structure for segmental bone defect regeneration in a novel sheep model. J Tissue Eng Regen Med. 2018;12(4):897–911.
2. Ye X, Li L, Lin Z, Yang W, Duan M, Chen L, et al. Integrating 3D-printed PHBV/Calcium sulfate hemihydrate scaffold and chitosan hydrogel for enhanced osteogenic property. Carbohydr Polym. 2018;202:106–14.
3. Lu Y, Li L, Zhu Y, Wang X, Li M, Lin Z, et al. Multifunctional copper-containing carboxymethyl chitosan/alginate scaffolds for eradicating clinical bacterial infection and promoting bone formation. ACS Appl Mater Interfaces. 2018;10(1):127–38.
4. Borrelli J Jr, Prickett WD, Ricci WM. Treatment of nonunions and osseous defects with bone graft and calcium sulfate. Clin Orthop Relat Res. 2003;411:245–54.
5. Lasanianos NG, Kanakaris NK, Giannoudis PVJO. Current management of long bone large segmental defects. Orthop Trauma. 2010;24(2):149–63.
6. Lu Y, Li L, Li M, Lin Z, Wang L, Zhang Y, et al. Zero-dimensional carbon dots enhance bone regeneration, osteosarcoma ablation, and clinical bacterial eradication. Bioconjug Chem. 2018;29(9):2982–93.
7. Mauffrey C, Barlow BT, Smith W. Management of segmental bone defects. J Am Acad Orthop Surg. 2015;23(3):143–53.
8. Halim AS, Chai SC, Wan Ismail WF, Wan Azman WS, Mat Saad AZ, Wan Z. Long-term outcome of free fibula osteocutaneous flap and massive allograft in the reconstruction of long bone defect. J Plast Reconstr Aesthet Surg. 2015;68(12):1755–62.
9. Grover V, Kapoor A, Malhotra R, Sachdeva S. Bone allografts: a review of safety and efficacy. Indian J Dent Res. 2011;22(3):496.
10. Tosounidis TH, Giannoudis PV. Biological facet of segmental bone loss reconstruction. J Orthop Trauma. 2017;31(Suppl 5):S27–S31.
11. Sarkar MR, Augat P, Shefelbine SJ, Schorlemmer S, Huber-Lang M, Claes L, et al. Bone formation in a long bone defect model using a platelet-rich plasma-loaded collagen scaffold. Biomaterials. 2006;27(9):1817–23.
12. Egol KA, Nauth A, Lee M, Pape H-C, Watson JT, Borrelli J. Bone grafting: sourcing, timing, strategies, and alternatives. J Orthop Trauma. 2015;29(Suppl 12):S10–S14.
13. Jahan K, Manickam G, Tabrizian M, Murshed M. In vitro and in vivo investigation of osteogenic properties of self-contained phosphate-releasing injectable purine-crosslinked chitosan-hydroxyapatite constructs. Sci Rep. 2020;10(1):11603.
14. Jones DB Jr, Burger H, Bishop AT, Shin AY. Treatment of scaphoid waist nonunions with an avascular proximal pole and carpal collapse. A comparison of two vascularized bone grafts. J Bone Joint Surg Am. 2008;90(12):2616–25.
15. Jones AL, Bucholz RW, Bosse MJ, Mirza SK, Lyon TR, Webb LX, et al. Group, Recombinant human BMP-2 and allograft compared with autogenous bone graft for reconstruction of diaphyseal tibial fractures with cortical defects. A randomized, controlled trial. J Bone Joint Surg Am. 2006;88(7):1431–41.
16. Wang EA, Rosen V, D'Alessandro JS, Bauduy M, Cordes P, Harada T, et al. Recombinant human bone morphogenetic protein induces bone formation. Proc Natl Acad Sci U S A. 1990;87(6):2220–4.

17. Rodriguez IA, Growney Kalaf EA, Bowlin GL, Sell SA. Platelet-rich plasma in bone regeneration: engineering the delivery for improved clinical efficacy. Biomed Res Int. 2014;2014:392398.
18. Roffi A, Di Matteo B, Krishnakumar GS, Kon E, Filardo G. Platelet-rich plasma for the treatment of bone defects: from preclinical rational to evidence in the clinical practice. A systematic review. Int Orthop. 2017;41(2):221–37.
19. Hall MP, Band PA, Meislin RJ, Jazrawi LM, Cardone DA. Platelet-rich plasma: current concepts and application in sports medicine. J Am Acad Orthop Surg. 2009;17(10):602–8.
20. Chatterjea A, Yuan H, Fennema E, Burer R, Chatterjea S, Garritsen H, et al. Engineering new bone via a minimally invasive route using human bone marrow-derived stromal cell aggregates, microceramic particles, and human platelet-rich plasma gel. Tissue Eng Part A. 2013;19(3–4):340–9.
21. DurmuŞlar MC, Alpaslan C, Alpaslan G, Çakır M. Clinical and radiographic evaluation of the efficacy of platelet-rich plasma combined with hydroxyapatite bone graft substitutes in the treatment of intra-bony defects in maxillofacial region. Acta Odontol Scand. 2014;72(8):948–53.
22. Chen TL, Lu HJ, Liu GQ, Tang DH, Zhang XH, Pan ZL, et al. Effect of autologous platelet-rich plasma in combination with bovine porous bone mineral and bio-guide membrane on bone regeneration in mandible bicortical bony defects. J Craniofac Surg. 2014;25(1):215–23.
23. Huang Z, Wang W, Wang Q, Hojnacki T, Wang Y, Fu Y, et al. Coaxial nanofiber scaffold with super-active platelet lysate to accelerate the repair of bone defects. RSC Adv. 2020;10(59):35776–86.
24. Galanis V, Fiska A, Kapetanakis S, Kazakos K, Demetriou T. Effect of platelet-rich plasma combined with demineralised bone matrix on bone healing in rabbit ulnar defects. Singapore Med J. 2017;58(9):551–6.
25. Garrett IR, Gutierrez GE, Rossini G, Nyman J, McCluskey B, Flores A, et al. Locally delivered lovastatin nanoparticles enhance fracture healing in rats. J Orthop Res. 2007;25(10):1351–7.
26. Keating JF, Simpson AH, Robinson CM. The management of fractures with bone loss. J Bone Joint Surg Br. 2005;87(2):142–50.
27. Grageda E. Platelet-rich plasma and bone graft materials: a review and a standardized research protocol. Implant Dent. 2004;13(4):301–9.
28. Butterfield KJ, Bennett J, Gronowicz G, Adams D. Effect of platelet-rich plasma with autogenous bone graft for maxillary sinus augmentation in a rabbit model. J Oral Maxillofac Surg. 2005;63(3):370–6.
29. Gao SY, Lin RB, Huang SH, Liang YJ, Li X, Zhang SE, et al. PDGF-BB exhibited therapeutic effects on rat model of bisphosphonate-related osteonecrosis of the jaw by enhancing angiogenesis and osteogenesis. Bone. 2021;144:115117.
30. Czapla J, Matuszczak S, Kulik K, Wiśniewska E, Pilny E, Jarosz-Biej M, et al. The effect of culture media on large-scale expansion and characteristic of adipose tissue-derived mesenchymal stromal cells. Stem Cell Res Ther. 2019;10(1):235.
31. Marini M, Bertolai R, Manetti M, Sgambati E. A case of mandible hypoplasia treated with autologous bone graft from mandibular symphysis: Expression of VEGF and receptors in bone regeneration. Acta Histochem. 2016;118(6):652–6.
32. Wittbjer J, Palmer B, Thorngren KG. Osteogenetic properties of reimplanted decalcified and undecalcified autologous bone in the rabbit radius. Scand J Plast Reconstr Surg. 1982;16(3):239–44.
33. Concannon MJ, Boschert MT, Puckett CL. Bone induction using demineralized bone in the rabbit femur: a long-term study. Plast Reconstr Surg. 1997;99(7):1983–8.
34. Song Y, Lin K, He S, Wang C, Zhang S, Li D, et al. Nano-biphasic calcium phosphate/polyvinyl alcohol composites with enhanced bioactivity for bone repair via low-temperature three-dimensional printing and loading with platelet-rich fibrin. Int J Nanomedicine. 2018;13:505–23.
35. Intini G. The use of platelet-rich plasma in bone reconstruction therapy. Biomaterials. 2009;30(28):4956–66.
36. Wei B, Huang C, Zhao M, Li P, Gao X, Kong J, et al. Effect of mesenchymal stem cells and platelet-rich plasma on the bone healing of ovariectomized rats. Stem Cells Int. 2016;2016:9458396.
37. Kasten P, Vogel J, Geiger F, Niemeyer P, Luginbühl R, Szalay K. The effect of platelet-rich plasma on healing in critical-size long-bone defects. Biomaterials. 2008;29(29):3983–92.

How to cite this article: Wang Q, Huang Z, Huang X, Zhang T, Wang W. Reparative effect of super active platelet combined with allogeneic bone for large bone defects. *Artif Organs*. 2021;00:1–10. https://doi.org/10.1111/aor.14002